IOPscience iopscience.iop.org

Home Search Collections Journals About Contact us My IOPscience

Highest Occupied Molecular Orbital of Cyclopentanone by Binary (e, 2e) Spectroscopy

This article has been downloaded from IOPscience. Please scroll down to see the full text article.

2006 Chinese Phys. Lett. 23 583

(http://iopscience.iop.org/0256-307X/23/3/016)

View the table of contents for this issue, or go to the journal homepage for more

Download details:
IP Address: 166.111.26.181
The article was downloaded on 06/05/2011 at 07:04

Please note that terms and conditions apply.

Highest Occupied Molecular Orbital of Cyclopentanone by Binary (e, 2e) Spectroscopy *

ZHANG Shu-Feng(张书锋), NING Chuan-Gang(宁传刚), DENG Jing-Kang(邓景康)**,
REN Xue-Guang(任雪光), SU Guo-Lin(苏国林), YANG Tie-Cheng(杨铁成), HUANG Yan-Ru(黄艳茹)
Department of Physics and Key Laboratory of Atomic and Molecular Nanosciences of MOE, Tsinghua University, Beijing 100084

(Received 16 November 2005)

We report the first measurements of the momentum profiles of highest occupied molecular orbital (HOMO) and the complete valence shell binding energy spectra of cyclopentanone with impact energies of 600 and 1200 eV by a binary (e, 2e) spectrometer. The experimental momentum profiles of the HOMO orbital are compared with the theoretical momentum distribution calculated using the Hartree–Fock and density functional theory methods with various basis sets. However, none of these calculations gives a completely satisfactory description of the momentum distributions of the HOMO $7b_2$. The inadequacy of the calculations could result in the intensity difference of the second maximum at $p \sim 1.2$ a.u. between the experiment and the theory. The discrepancy between experimental and theoretical data in the low-momentum region is explained with the distorted wave effect.

PACS: 33. 15. Ry, 34. 80. Gs, 36. 20,Kd

Electron momentum spectroscopy (EMS), based on a binary (e, 2e) ionization reaction, has been shown to be a powerful and informative experimental tool for the study of the electronic structure of atoms, molecules, biomolecules and condensed matter.[1−3] The unique ability of EMS to measure electron momentum distributions of individual molecular orbitals has made it become an important experimental technique for studying electronic structures. The momentum distribution information obtained by EMS provides a powerful proof for evaluating the quality of quantum chemical calculations[1,3] at the Hartree–Fock (HF) level and also of correlated treatments such as configuration interaction methods and density functional theory (DFT). The HOMO is very important for many chemical and physical properties, such as structure-reactivity relations, molecular similarity and dissimilarity. Cooper and Allan suggested that it would be interesting and potentially fruitful to make HOMO and/or LUMO (lowest unoccupied molecular orbital) comparisons as a measure of molecular discrimination.[4]

In this Letter, we report the complete valence shell binding energy spectra (5–40 eV) of cyclopentanone ($(CH_2)_4CO$) and its HOMO electron momentum profile using EMS at impact electron energies of 600 and 1200 eV plus binding energy with a symmetric noncoplanar geometry. Cyclopentanone is an important intermediate useful in the synthesis of flavour and fragrance chemicals, pharmaceuticals, insecticides, rubber chemicals, and biologically active compounds. It can also be used as a solvent. Cyclopentanone is a member of a series of five-membered ring compounds, its HOMO is mainly concentrated on the lone pair orbital of the oxygen atom of the carbonyl group.[5] The electronic states of cyclopentanone have been investigated by photoelectron spectroscopy (PES) and various theoretical methods.[5−10] Our experimental momentum profiles are compared with HF and DFT calculations using various basis sets. However, none of these calculations gives a completely satisfactory description of the momentum distribution of the HOMO $7b_2$. We have explained the discrepancy between the experiment and the theory. To the best of our knowledge, this work is the first EMS study of cyclopentanone.

Recently we have developed a new type EMS spectrometer[11,12] with two orders higher efficiency than typical energy dispersive multichannel electron momentum spectrometers.[13] The basic principle of EMS is an impact ionization reaction, where the gas phase target molecules are ionized by a high energy electron beam.[1−3] The outgoing electrons (scattered and ionized) are angle and energy selected by a toroidal energy analyser and then detected in coincidence. The experimental geometry is symmetric noncoplanar, i.e. the two outgoing electrons are selected to have equal polar angles ($\theta_1 = \theta_2 = 45°$, angle between the outgoing electron direction and the incoming electron beam direction). The azimuthal angles (ϕ, angle between the outgoing electron direction in the plane normal to the beam direction, and $\phi = 0°$ is the scattering plane) from $-38°$ to $38°$ are simultaneously measured, so the detection efficiency is much higher. All binding energy spectra (BES) at different angles are collected at the same time, so the effects of instabilities of the electron beam and gas sample intensity are greatly reduced.

* Supported by the National Natural Science Foundation of China under Grant No 10575062, and the Specialized Research Fund for the Doctoral Programme of Higher Education of China under Grant No 20050003084.

** To whom correspondence should be addressed. Email: djk-dmp@mail.tsinghua.edu.cn

©2005 Chinese Physical Society and IOP Publishing Ltd

A profile of differential cross section versus recoil momentum for each energy resolved state of the target molecules is obtained from these BES at different ϕ angles. Under the binary encounter requirements of high impact energy and high-momentum transfer, the initial momentum p of the knocked-out electron can be given by

$$p = \{(2p_1 \cos\theta_1 - p_0)^2 + [2p_1 \sin\theta_1 \sin(\phi/2)]^2\}^{1/2}, \quad (1)$$

where p_1, p_2 ($p_1 = p_2$) are the momenta of each of the two outgoing electrons, and p_0 is the momentum of the incident electron.

Theoretical orbital momentum densities are calculated within the plane wave impulse approximation. Using the Born-Oppenheimer approximation for the target and ion wave function, the EMS orbital cross-section σ, for randomly oriented molecules and unresolved rotational and vibrational states, is given by[3]

$$\sigma = K \int d\Omega |\langle p\, \Psi_f^{N-1} |\, \Psi_i^N \rangle|^2, \quad (2)$$

where K is a kinematical factor which is essentially constant in the present experimental arrangement, Ψ_f^{N-1} and Ψ_i^N are the electronic many-body wave functions for the final ($(N-1)$ electron) ion and target (N electron) ground states, and p is the momentum of the target electron at the instant of ionization. The $\int d\Omega$ denotes an integral over all angles (spherical averaging) due to averaging over all initial rotational states. The average over the initial vibrational states is well approximated by evaluating orbitals at the equilibrium geometry of the molecule. Final rotational and vibrational states are eliminated by closure.[3]

The momentum space target-ion overlap $\langle p\, \Psi_f^{N-1} |\, \Psi_i^N \rangle$ can be evaluated using configuration interaction descriptions of the many-body wave function, but usually the weak-coupling approximation is made.[3] Here, the target-ion overlap is replaced by the relevant orbital of, typically the Hartree–Fock or Kohn–Sham [14] ground state Φ_0, multiplied by a spectroscopic amplitude. With these approximations Eq. (2) reduces to

$$\sigma \propto S_i^f \int d\Omega |\, \Psi_j(\boldsymbol{p})|^2, \quad (3)$$

where $\Psi_j(\boldsymbol{p})$ is the one-electron momentum space orbital wave function for the jth electron, corresponding to the orbital in the neutral initial state immediately prior to ionization. The quantity $\Psi_j(\boldsymbol{p})$ is the Fourier transform of the more familiar one-electron position space orbital wave function $\Psi_j(\boldsymbol{r})$. The quantity S_i^f is the spectroscopic factor or pole strength and is the probability of the ionization event producing a $(\psi_j)^{-1}$ one-hole configuration of the final ion state, $|\Psi_f^{N-1}\rangle$. Equation (3) explicitly shows the relationship between the orbital momentum density and imaging capability of the EMS.

In EMS, the individual orbitals are selected by the binding (or ionization) energy. With the double toroidal energy analyser used in the present work, BESs are collected at different azimuthal angles ϕ at the same time. Momentum distributions as a function of angle ϕ are obtained by deconvolution of these BES using Gaussian functions located at each ionization energy. The widths of the Gaussian functions can be determined from a consideration of published PES vibronic manifolds and the instrumental energy resolution. For each ionization process, the set of areas of fitted peaks is plotted as a function of momentum which is calculated from ϕ using Eq. (1). To compare the experimental momentum distributions with the relative cross sections calculated as a function of momentum using Eq. (2), the effects of the finite spectrometer angular resolution in both θ and ϕ ($\Delta\theta \approx \pm 0.7^\circ$ and $\Delta\phi \approx \pm 1.9^\circ$) should be included. This is achieved with the Gaussian method[15] in this work. After momentum resolution folding, the calculations (Eqs. (2) and (3)) are referred to as a theoretical momentum profile.

In our experiments the "binning" mode[16] is employed for collecting coincidence binding energy spectra. The sample of cyclopentanone measured in this work is $\geq 99.0\%$ purity, and is used without any purification. No impurities are observed in the BES.

Cyclopentanone has C_{2v} point group symmetry and its electronic configuration in the ground state can be written as

$$(core)^{12}(5a_1)^2(6a_1)^2(3b_2)^2(7a_1)^2(4b_2)^2(8a_1)^2(1b_1)^2$$
$$(1a_2)^2(9a_1)^2(2b_1)^2(5b_2)^2(10a_1)^2(6b_2)^2(11a_1)^2(3b_1)^2$$
$$(2a_2)^2(7b_2)^2.$$

In the ground state, there are 46 electrons arranged in 23 double-occupied orbitals in the independent particle description. The binding energy for each valence orbital is obtained from the He (II) PES data.[10] In the PES work, the vertical ionization potential of the $7b_2$ HOMO is 9.3 eV, and the $(2a_2 + 3b_1 + 11a_1 + 6b_2)$, $(10a_1 + 5b_2 + 2b_1 + 9a_1)$, $1a_2$, $1b_1, 8a_1, 4b_2$, $7a_1$ and $3b_2$ orbitals are determined to be $(11.5 - 12.9)$, $(13.5 - 15.0)$, 16.1, 16.7, 17.7, 19.4, 22.0 and 23.2 eV, respectively.

To obtain the experimental momentum profiles, these BESs are collected at ϕ angles with steps of 1°. The BESs of cyclopentanone measured at the azimuthal angle $\phi = 1^\circ$ and $\phi = 10^\circ$ are shown in Fig. 1. The BESs are fitted with a series of individual Gaussian peaks whose widths are combinations of the EMS instrumental energy resolution (full width at half maximum, FWHM=1.1 and 1.3 eV at impact energies of 600 and 1200 eV, respectively) and the corresponding Franck–Condon widths derived from the high-resolution PES data.[10] The dotted lines fitted to Gaussian curves indicate the individual peaks, while the solid line represents their sum.

In the present EMS work, 11 structures can be identified in the binding energy spectra of Fig. 1. The

vertical ionization potential of the HOMO $7b_2$ is determined to be 9.30 eV. Due to the small energy separation among these orbitals, the averaged ionization potentials for $(2a_2+3b_1+11a_1+6b_2)$, $(5b_2+2b_1+9a_1)$ and $(1a_2+1b_1)$ are determined to be 12.25, 14.4 and 16.2 eV, respectively. For $10a_1$, $8a_1$, $4b_2$, $7a_1$, $3b_2$, $6a_1$, and $5a_1$ orbitals, the ionization potentials are given to be 13.8, 17.55, 19.4, 22.0, 23.2, 25.8, and 31.3 eV respectively. The peak for the $10a_1$ orbital in the BES at $\phi = 10^\circ$ is too weak to be seen because $10a_1$ has an s-type momentum distribution and its cross section at $\phi = 10^\circ$ is close to zero. It should be noted that the average ionization energy in this work is predetermined by PES, and then it is slightly shifted to have a best fitting of the summed energy spectra. The differences among FWHMs of these peaks are due to the vibrational broadening. The very broad structure with a peak at 27.3 eV in Fig. 1 is due to the residual background and closely spaced satellite lines in the high energy region. For two-dimensional detectors, the background could not be clearly subtracted due to the marginal image distortion and the coincidence time spectrum structures.

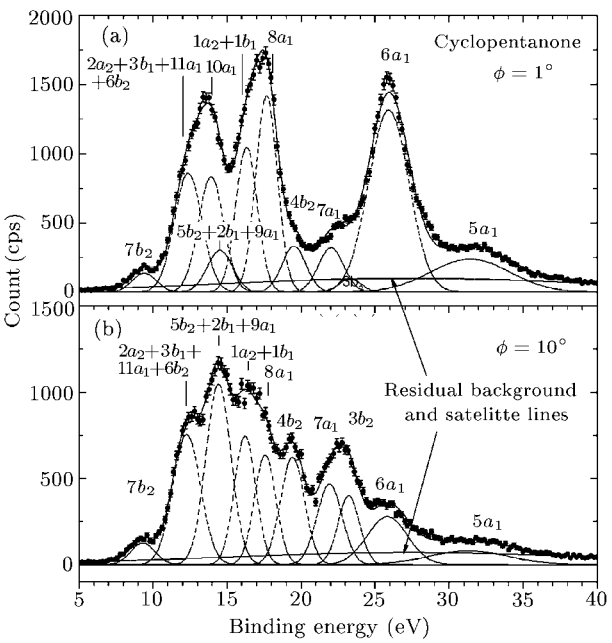

Fig. 1. Binding energy spectra of cyclopentanone at (a) $\phi = 1^\circ$ and (b) $\phi = 10^\circ$ with 1200 eV impact energy plus binding energy. The dashed and solid lines represent individual and summed Gaussian fits, respectively.

The experimental momentum profiles are extracted by deconvolution of the same peak from the BES at different azimuthal angles. As shown in Fig. 2, the experimental momentum profiles (XMPs) of cyclopentanone HOMO $7b_2$ with impact energies of 600 and 1200 eV are compared with various theoretical momentum profiles (TMPs), which have incorporated the instrumental angular resolutions. The experimental data and theoretical values have been placed on a common intensity scale by normalizing the experimental to the theoretical momentum profile calculated by the DFT method using B3LYP hybrid functional and the augmented correlation consistent polarized valence triple zeta (aug-cc-pVTZ) basis set for the $7b_2$ orbital. The difference between theoretical distributions at 600 and 1200 eV is due to the better experimental momentum resolution at lower impact energy. The calculations are carried out with the Gaussian program. It can be seen that HF (curve 1 with STO-3G basis set, curve 2 with 6-31G, curve 3 with 6-311++G**, and curve 4 with aug-cc-pVTZ) and DFT (B3LYP method, curve 5 with 6-31G basis set, curve 6 with 6-311++G**, and curve 7 with aug-cc-pVTZ) calculations do not well describe the experimental results in Figs. 2(a) and 2(b). The experimental data show a double "lobed" momentum distribution with peaks at about 0.4 a.u. and 1.2 a.u.. All the calculations indicate that the momentum distribution of the HOMO $7b_2$ has a double p-type character, which is the case as shown in our EMS experiment. However, different calculations give different relative intensities of the two peaks in momentum profiles. Larger basis sets give more accurate descriptions of XMPs, especially in the high-momentum region (above 1.0 a.u.). The small basis set HF calculations (curves 1, with STO-3G) give poor intensity in the low-momentum region and shift the position of the second maximum slightly to the high-momentum side compared with the XMPs. The intensity ratio of the first peak to the second peak is increased for the 6-31G and 6-311++G** calculations and it agrees better with the experimental data. Using the DFT-B3LYP calculation with the aug-cc-pVTZ basis set achieved a slightly better description of cyclopentanone HOMO momentum distribution in the intensity and position of maximum than other calculations. The shape of the reported momentum distribution of HOMO of cyclopentanone is similar to that of the acetone (CH_3COCH_3) HOMO $5b_2$ orbital[16] and the experimental results show some deviation from theoretical momentum profiles in both the cases. The HOMO $5b_2$ of acetone is mainly due to the lone pair oxygen $2p$ electrons.[16] Usually, HOMO orbitals are very diffuse in position space and they contribute the least to the total energy. Therefore, their outer diffuse regions are likely not well modelled by the self-consistent field variational method. Thus highly saturated basis sets including very diffuse functions are expected to be necessary to produce converged results particularly for HOMO momentum distribution. Intensity ratio of the first maximum to the second one depends strongly on the theoretical methods and basis sets selected, and even the DFT-B3LYP/aug-cc-pVTZ calculation can not reproduce nicely the experimental intensity ratio. The second peak of the theoretical momentum profile is noticeably higher than that from the experiment, as seen in Fig. 2(b). The inadequacy of the calculations might be the reason of the intensity difference of the second maximum between the experiment and theory. Further high level theoretical

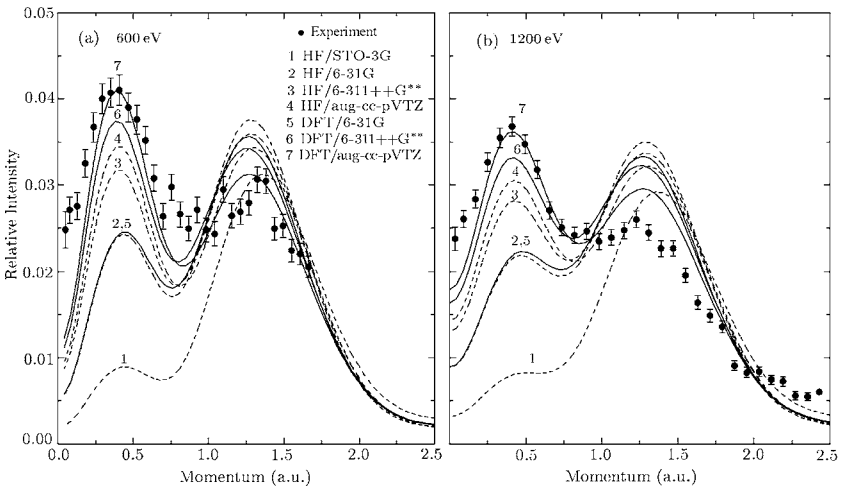

Fig. 2. Experimental and calculated momentum distributions for the HOMO $7b_2$ orbital of cyclopentanone with (a) 600 eV and (b) 1200 eV impact energy. The theoretical momentum profiles are calculated using HF (curves 1, 2, 3 and 4) and DFT-B3LYP (curve 5, 6 and 7).

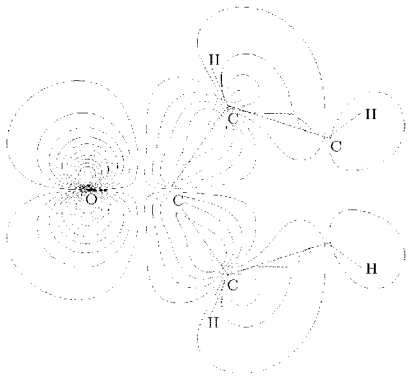

Fig. 3. Orbital wave function plot for the HOMO $7b_2$ orbital of cyclopentanone in the position space calculated using the HF method and the 6-311++G** basis set.

work may be required for the HOMO of cyclopentanone.

A possible explanation for the discrepancy in the low-momentum region between XMPs and TMPs is the distorted wave effect. The smaller momentum transfer might also come from the near nucleus region in some d-like orbitals, such as π^* orbital,[17−21] because the momentum is related to the gradient of the position space wavefunction: low momentum is consistent with the low gradient of the position space wavefunction. For d-like orbitals, the gradient of wavefunctions is very low in the region near the nucleus.[17] Thus the distorted wave effect will manifest more remarkably at lower momentum for d-like orbitals. The theoretical calculation shows that there is some extent π^* orbital in the cyclopentanone HOMO $7b_2$ (see Fig. 3). Such particular molecular orbital is similar to d-type atomic or π^* molecular orbital with regard to symmetry. Therefore the observed "turn up" effect in the low-momentum region of cyclopentanone $7b_2$ orbital momentum distributions is due to the distorted wave effect could be confirmed. To further confirm this explanation, the experiments are carried out at both 600 eV and 1200 eV. It is expected the discrepancy of 600 eV will become more evident than that of 1200 eV because the nucleus will distort the electron waves greater at lower impact energy according to the molecular collision theory. Consequently, it is found that the turn-up is larger at 600 eV than at 1200 eV in the region of momentum < 0.3 a.u. as illustrated in Figs. 2(a) and 2(b). The difference between experimental and B3LYP/aug-cc-pVTZ theoretical intensity, for example, at 0.1 a.u., is 0.012 for 600 eV, while is 0.006 for 1200 eV. Thus the distorted wave effect explanation predicts well the experimental trends. The quantitatively calculation for distorted wave effect in molecular orbital is still a challenge for theorists because of the complexity of the multi-center system.

References

[1] McCarthy I E and Weigold E 1991 *Rep. Prog. Phys.* **54** 789

[2] Coplan M A, Moore J H and Doering J P 1994 *Rev. Mod. Phys.* **66** 985

[3] Weigold E and McCarthy I E 1999 *Electron Momentum Spectroscopy* (New York: Kluwer)

[4] Cooper D L and Allan A L 1992 *J. Am. Chem. Soc.* **114** 4773

[5] Bain A D and Frost D C 1973 *Can. J. Chem.* **51** 1245

[6] Kosmidis C, Philis J G and Tzallas P 1999 *Phys. Chem. Chem. Phys.* **1** 2945

[7] Vaz P D and Ribeiro-Claro P J A 2003 *J. Phys. Chem.* A **107** 6301

[8] Furuya K, Yamamoto E, Jinbou Y and Ogawa T 1994 *J. Electron Spectrosc. Relat. Phenom.* **73** 59

[9] Chadwick D, Frost D C and Weiler L 1971 *J. Am. Chem. Soc.* **93** 4320

[10] Bieri G, Åsbrink L and Niessen W von 1982 *J. Electron Spectrosc. Relat. Phenom.* **27** 129

[11] Ren X G, Ning C G, Deng J K, Zhang S F, Su G L, Huang F and Li G Q 2005 *Rev. Sci. Instrum.* **76** 063103

[12] Ren X G, Ning C G, Deng J K, Zhang S F, Su G L, Li B and Chen X J 2005 *Chin. Phys. Lett.* **22** 1382

[13] Deng JK, Li G Q, He Y, Huang J D, Deng H, Wang X D, Wang F, Zhang Y A, Ning C G, Gao N F, Wang Y, Chen X J and Zheng Y 2001 *J. Chem. Phys.* **114** 882

[14] Kohn W and Sham L J 1965 *Phys. Rev.* A **140** 1133

[15] MiGdall J N, Coplan M A and Hench D S et al 1981 *Chem. Phys.* **57** 141

[16] Zheng Y, Neville J J, Brion C E, Wang Y and Davidson E R 1994 *Chem. Phys.* **188** 109

[17] Brion C E, Zheng Y, Rolke J, Neville J J and Wang J 1998 *J. Phy. B: At. Mol. Opt. Phys.* **31** L223

[18] Deng J K, Li G Q, Huang J D, Wang F, Ning C G, Lu J, He Y, Wang X D, Zhang Y A, Gao H, Wang Y and Zheng Y 2002 *Chin. Phys. Lett.* **19** 47

[19] Ren X G, Ning C G, Deng J K, Zhang S F, Su G L, Huang F and Li G Q 2005 *Phys. Rev. Lett.* **94** 163201

[20] Zhang X H, Chen X J, Xu C K, Jia C C, Yin X F, Shan X, Wei Z and Xu K Z 2004 *Chem. Phys.* **299** 17

[21] Wu X J, Chen X J, Chen L Q, Li Z J, Yang X F, Shan X, Zheng Y Y and Xu K Z 2005 *Chin. Phys. Lett.* **22** 1649